Eur. Phys. J. B **46**, 169–176 (2005)
DOI: 10.1140/epjb/e2005-00226-0

THE EUROPEAN
PHYSICAL JOURNAL B

Sound wave anomalies in superconducting compounds

B. Lüthi[1,a], S. Zherlitsyn[2], and B. Wolf[1]

[1] Physikalisches Institut, Universität Frankfurt, 60054 Frankfurt, Germany
[2] Forschungszentrum Rossendorf, 01328 Dresden, Germany

Received 18 November 2004
Published online 19 July 2005 –

Abstract. Temperature dependence of the elastic constants in the superconducting state is described on the basis of the Ginsburg-Landau theory. This approach shows very general character and allows to describe quantitative renormalization of the elastic constants in the superconducting state for different materials including non-conventional superconductors. Various examples (A-15 compounds, Chevrel compounds, $CeRu_2$, $Ba_{0.63}K_{0.37}BiO_3$, $Yb_3Rh_4Sn_{13}$, $Ca_3Rh_4Sn_{13}$, HfV_2, some heavy fermion compounds and Sr_2RuO_4) are given.

PACS. 74.25.Ld Mechanical and acoustical properties, elasticity, and ultrasonic attenuation

1 Introduction

Sound wave effects in superconducting elements like Sn, Pb, Nb etc are well documented. In superconducting compounds like A-15 material, Chevrel phase structures, stannides, high temperature superconductors or heavy fermion systems there is a rich variety of ultrasonic effects (see e.g. Ref. [1]). In most cases they have not been quantitatively described. Here we want to give a simple phenomenological description of these effects using the Ginzburg-Landau theory of superconductivity. In most cases of ultrasonic experiments in these compounds we are in the limit $ql_e \ll 1$ (q wave number of sound wave, l_e electronic mean free path). Therefore we notice pronounced sound velocity effects and only in very rare cases typical sound attenuation effects due to contribution of conduction electrons.

In the next section we derive the necessary formulas for longitudinal and transverse sound velocities or elastic constants for the model in question. Our approach is similar to the one, first given by Testardi [2]. In the following chapter we apply derived formulas for fits to the various experimental results. In most cases these fits give a satisfactory agreement with the experimental data. We treat only the field free case $B = 0$ in this paper.

2 Calculation of the elastic constants: Ginzburg - Landau model

Following the Landau theory of the second order phase transitions we start with the order parameter expansion of the free energy density:

$$\Delta F = (a/2)|\eta|^2 + (b/4)|\eta|^4 + \dots \quad (1)$$

$\Delta F = F - F_o$ is a change of the free energy in the superconducting state. Here we have to use for the complex superconducting order parameter (OP) the absolute value $|\eta|$. In the Ginsburg-Landau theory $|\eta|^2$ is proportional to the density of Cooper pairs. In the case of unconventional superconductors the OP can have two or more components. $dF/d|\eta| = 0$ gives the equilibrium value

$$|\eta|^2 = -a/b = a_o(T_c - T)/b, \quad (2)$$

where we have used the Landau Ansatz $a = a_o(T - T_c)$. Here T is temperature and T_c is the temperature of the superconducting phase transition, $a_0 > 0$ is a constant. Substituting the OP back into equation (1) gives for the free energy density

$$\Delta F = -a_o^2/4b(T - T_c)^2 = -\Phi_o(1 - T/T_c)^2. \quad (3)$$

This is valid for temperatures $T < T_c$. Here we have introduced $\Phi_o = a_o^2 T_c^2/4b$ which we can interpret as the $T = 0$ condensation energy density. For the following we assume that $\Phi_o(\varepsilon)$ and $T_c(\varepsilon)$ are strain dependent. Then we can calculate the elastic constants, using the symmetry strain ε_Γ, with $c_\Gamma = d^2F/d\varepsilon_\Gamma^2$:

$$\begin{aligned} c_\Gamma = c_\Gamma^o &- 2(\partial T_c/\partial\varepsilon_\Gamma)^2 \Phi_o T/T_c^3(-2 + 3T/T_c) \\ &- 2(\partial^2 T_c/\partial\varepsilon_\Gamma^2)\Phi_o T/T_c^2(1 - T/T_c) \\ &- 4(\partial T_c/\partial\varepsilon_\Gamma)(\partial\Phi_o/\partial\varepsilon_\Gamma)T/T_c^2(1 - T/T_c) \\ &- \partial^2\Phi_o/\partial\varepsilon_\Gamma^2(1 - T/T_c)^2. \end{aligned} \quad (4)$$

Here c_Γ^o is the background elastic constant, Γ is the symmetry label for the elastic constant and the corresponding strain. The four terms involving the different strain derivatives we discuss in the following.

[a] e-mail: luethi@physik.uni-frankfurt.de

Table 1. s.c. transition temp. T_c, Sommerfeld parameter γ in (mJ/mol)K^{-2}, mass density ρ, elastic constants c_{ij} at $T = 200$ K in 10^{11}erg/cm^3, coupling constants A_1, A_2.

Material	T_c K	γ	Density g/cm^3	c_{11}	$\frac{(c_{11}-c_{12})}{2}$	c_{44}	A_1 $\times 10^{-3}$	A_2 $\times 10^{-3}$	$\lvert(\Delta c/c_0)_{OP}\rvert$	Acoustic mode
V_3Ge	6.0	31	6.87	29.3	9.2	7.03	1	0.46		$c_{11}-c_{12}$
V_3Si	17.0	59	5.86	28.7	8.34	8.09				
Nb_3Sn	18.2	63	8.80	24.5	6.8	7.66				
$PbMo_6S_8$	13.2	105	6.3	9.29^b	10.75^b		-	–6.5		T
							-	–5.5		L
$Eu_{0.6}Sn_{0.4}Mo_6S_8Br_{0.1}$	7.8		11.5	2.18^b	3.13^b		-	–2.55		T
								–4.5		L
$CeRu_2$	6.1	50	10.6	13.85	2.29	0.57	4	1.8		$c_{11}-c_{12}$
							0.08	–0.015		c_{11}
$Ba_{.63}$ $K_{.37}$ BiO_3	31						2.1	–0.075		c_{11}
$Yb_3Rh_4Sn_{13}$	6.5		8.9	12.62	2.93	2.05				
$Ca_3Rh_4Sn_{13}$	7.1		8.3	13.91	3.29	1.86	0.5	–4.5		c_L
HfV_2	9.0	58.1	9.3	12.8	1.3	1.7			8.4×10^{-5}	c_L
UPt_3	0.54	450	19.40	32.10	9.30	3.90			5.6×10^{-5}	c_{11}
URu_2Si_2	1.40	120	10.01	25.51	10.40	13.34			12×10^{-5}	c_{11}
$CeCu_2Si_2$	0.50^a	600	6.40	17.10	0.95	4.70			5×10^{-5}	c_{11}
Sr_2RuO_4	1.42	38					0.55	0.25	1.3×10^{-4}	c_{11}
							0.118	0.062	8×10^{-6}	c_{66}
							0.0726	0.033	5.5×10^{-6}	c_{44}
							1.54	0.7	1.8×10^{-4}	$c_{11}-c_{12}$

[a]- T_c without A-phase.
[b]- c_L, c_T

In order to illustrate the significance of the various terms in equation (4) one can expand the Landau free energy density [see Eq. (3)] further with the strain terms included. By expanding $T_c(\varepsilon)$ and $\Phi_o(\varepsilon)$, in addition to the Landau free energy ΔF_L of equation (1) the additional terms are obtained:

$$F_{sp} = g_\Gamma \varepsilon_\Gamma |\eta|^2_\Gamma + g'_\Gamma \varepsilon_\Gamma |\eta|^4_\Gamma + h_\Gamma \varepsilon^2_\Gamma |\eta|^2_\Gamma + h'_\Gamma \varepsilon^2_\Gamma |\eta|^4_\Gamma + \ldots \tag{5}$$

Here we assume that these terms, linear and quadratic in the strain ε_Γ, exist for the symmetry Γ. The coupling constants g, g', h and h' can be related to the strain derivatives of T_c and Φ_o. These relations are described in the Appendix.

For high symmetry directions shear waves do not couple in lowest order because $\partial T_c/\partial\varepsilon_{sh} = \partial T_c/\partial(-\varepsilon_{sh}) = 0$. This was noted by Pippard [3]. This no longer holds true in cases of a multidimensional order parameters as occurs for e.g. in heavy fermion compounds. Higher order terms involving $\partial^2 T_c/\partial\varepsilon^2$ and other derivatives of Φ_o in equation (4) are also possible for shear waves.

3 Fit-procedure of experimental results

We want to fit equation (4) to very different superconductors. They include A-15 compounds, Chevrel phase materials, stannides, $CeRu_2$, HfV_2, $Ba_{1-x}K_xBiO_3$, Sr_2RuO_4 and heavy fermions. The experimental results are taken from the literature. In Table 1 we collect relevant data for the different superconductors investigated. We write equation (4) in the form

$$\Delta c/c_o = -\Big[2((\partial T_c/\partial\varepsilon)/T_c)^2(\Phi_o/c_o)F_o(T) + A_1F_1(T) + A_2F_2(T)\Big] \tag{6}$$

with $F_o = (T/T_c)(-2 + 3T/T_c)$ $\quad F_1 = T/T_c(1 - T/T_c)$ $F_2 = (1 - T/T_c)^2$.

The first term in equation (6) is the order parameter coupling discussed in the Appendix with $g = (a_o/2)\partial T_c/\partial\varepsilon$. For the following two terms we get for the coefficients A_1, A_2 the expressions

$$c_oA_1 = 2\partial^2T_c/\partial\varepsilon^2\Phi_o/T_c + 4/T_c\partial T_c/\partial\varepsilon\partial\Phi_o/\partial\varepsilon$$
$$A_2 = (\partial^2\Phi_o/\partial\varepsilon^2)/c_o). \tag{7}$$

Note that A_1 and A_2 and also F_i are dimensionless. If the first term (with g_Γ) of the strain-order parameter coupling expressions of equation (5) is negligible, the first term in equation (6) does not contribute. The term strain-order parameter coupling follows directly from the Ginzburg Landau treatment equation (5). It does not involve only $dT_c/d\varepsilon$ but also higher terms (g'_Γ and h'_Γ). Since A_1 involves two terms and A_2 also derivatives of Φ_o it is best

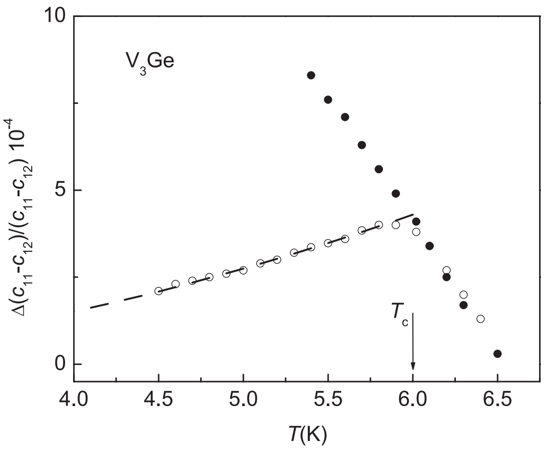

Fig. 1. V_3Ge : Temperature dependence of the $c_{11} - c_{12}$ mode near T_c [4]. Empty circles present measurements at $B = 0$, filled circles – measurements at $B = 2.3$ T. In the last case the sample stays in the normal state. Dashed line is a fit with equation (6) (see text for details).

to quote the $A_{1,2}$ values. Since with this survey we would like to stimulate microscopic theories of these effects, we just quote the A-values and the experimental $\Delta c/c_o$ values together with other physical quantities for the different superconductors in Table 1.

3.1 A-15 compounds

These superconductors were analysed already by Testardi (see Ref. [2]). In this review a relation between a structural instability and superconductivity was elaborated, and corresponding behaviour of elastic constant in the superconducting state was studied. A-15 compounds have a cubic structure and had the highest critical temperature before the copper oxide high temperature superconductors were discovered. A characteristic feature of these compounds is a tetragonal structural instability. Relatively high superconducting transition temperature in these compounds has been related to the lattice anharmonicity because of this structural instability.

In the following we will discuss V_3Ge for which elastic constant data exist for $T < T_c$ [4]. In Figure 1 elastic constant data are shown for the $(c_{11} - c_{12})/2$ mode. Clearly this mode exhibits a temperature dependence which can be interpreted with equations (4, 6). The fit gives the following values for $A_1 = 10^{-3}$, $A_2 = 0.46 \times 10^{-3}$. In this case the experimental data exists only for a limited temperature range below T_c, from 4.5 K to 6 K. Therefore one cannot say whether the values of fit parameters are preserved at low temperatures.

Other A-15 compounds cannot easily be interpreted in this way because strong attenuation effects prevent measurements of symmetry modes for these materials. An example is Nb_3Sn [5] where the assumption of a constant bulk modulus had to be invoked and no anomalies were seen at the superconducting phase transition for $T < T_c$ presumably because of strong domain-wall stress effects due to the structural transition at $T_a = 45$ K.

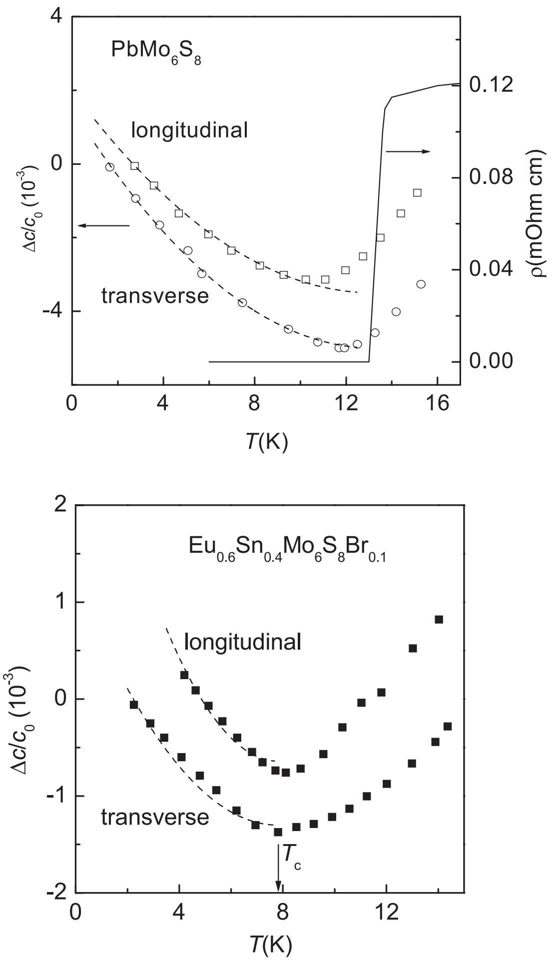

Fig. 2. $c_L(T)$, $c_T(T)$ and $\rho(T)$ for $PbMo_6S_8$ (a); $c_L(T)$ and $c_T(T)$ for $Eu_{0.6}Sn_{0.4}Mo_6S_8Br_{0.1}$ (b). Dashed lines give a fit with equation (6) with $F_1 = 0$ for $T \leq T_c$. Experimental results from reference [8].

3.2 Chevrel compounds

These are ternary molybdenum sulphide compounds with the general formula $MMoS_8$ where M stands for a large number of metals. The superconducting properties are mainly determined by the band structure of the Mo_6S_8 cluster. Single crystals of these materials are hardly available. Therefore most of the work was performed on sintered substances. Reviews on these compounds can be found in references [6,7].

In Figure 2a we show elastic constant data (longitudinal and transverse) for $PbMo_6S_8$ [8]. The electrical resistivity is also given in the figure ($T_c = 13.2$ K). A fit to the measured elastic constants with only the function $F_2(T)$ reproduces the temperature dependence very well. In Figure 2b we give likewise the results for the other Chevrel compound $Eu_{0.6}Sn_{0.4}Mo_6S_8Br_{0.1}$ with $T_c = 7.8$ K. Again the fit involving only F_2 describes the experimental results (longitudinal and transverse) very well. The corresponding fit parameters are giving in Table 1.

Chevrel compounds exhibit in addition other pronounced acoustic effects: a softening of the elastic modes

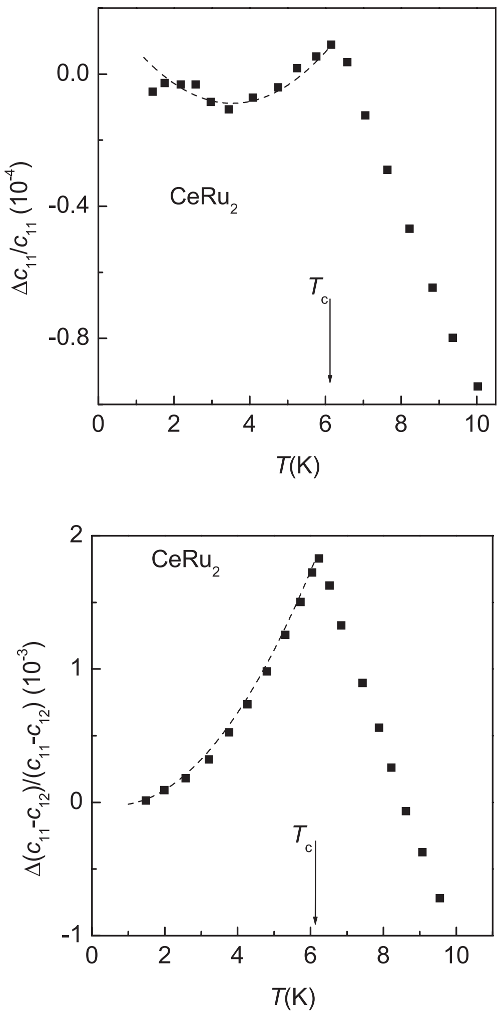

Fig. 3. c_{11} versus T (a) and $(c_{11} - c_{12})/2$ versus T (b) for $CeRu_2$. Dashed lines are fits with equation (6) for $T \leq T_c$. Experimental results from reference [10].

for $T > T_c$ and in magnetic fields for $T < T_c$ anomalies in velocity and attenuation which can be interpreted quantitatively with a vortices-strain coupling [8].

3.3 $CeRu_2$

This is a Laves phase compound with intriguing properties. It has a superconducting transition at $T_c = 6.3$ K. It was investigated with acoustic measurements by different groups [9–11]. The normal state elastic properties exhibit a pronounced softening for the $(c_{11} - c_{12})/2$ tetragonal mode. This is a precursor mode for a possible cubic-tetragonal phase transition for which the coupling constant is not quite large enough, however [10].

In Figure 3 we show data for the c_{11} and $(c_{11} - c_{12})/2$ modes in the low temperature region $T \leq 10$ K. For the longitudinal mode c_{11} we obtain a good fit with F_1 and F_2. We can also interpret the temperature behaviour of $c_{11} - c_{12}$ with our model. We get an equally good fit with F_1, F_2 (see dashed lines in Fig. 3).

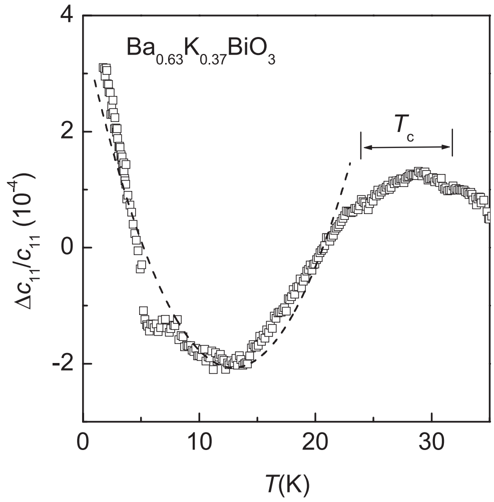

Fig. 4. $c_{11}(T)$ for $Ba_{0.63}$ $K_{0.37}$ BiO_3 [12]. Dashed line is a fit to equation (6) for $T \leq T_c$.

The magnetic field dependent behaviour of the elastic constants gives evidence for a pronounced peak effect. It was discussed with the so-called TAFF-model (thermally assisted flux flow) [10,11].

3.4 $Ba_{0.63}K_{0.37}BiO_3$

This high temperature copper-free superconductor has a superconducting transition at $T_c \approx 32$ K. The potassium concentration 0.37 is close to the phase boundary of cubic – orthogonal phases. The unique properties of this material depend strongly on the dynamics of the BiO_6 octahedra.

The acoustical properties were investigated by Zherlitsyn et al. [12]. Due to some inhomogeneous distribution of potassium in the crystal the superconducting phase transition might have some finite width. For our sample an onset of superconductivity was at 31.7 K, and the width of the transition was approximately 6 K. We found a strong softening of more than 10% for the c_{11} and c_{44} modes in the normal state. Some hysteretic behaviour of these modes around $T \sim 100$ K was interpreted with the anharmonic dynamics of the BiO_6 octahedra.

In Figure 4 we show the temperature dependence of the c_{11} mode in the vicinity of the superconducting phase transition. Below the superconducting transition we can fit the results adequately to equation (6) with the F_1 and F_2 terms of equation (6).

3.5 $Yb_3Rh_4Sn_{13}$ and $Ca_3Rh_4Sn_{13}$

These two ternary stannide compounds have transition temperatures of 6.5 K and 7.1 K respectively. They form a primitive cubic phase with two inequivalent sites for the Sn atoms: $Sn(1)Yb_3Rh_4Sn(2)_{12}$ with Sn(1) forming a A-15 type sublattice. The superconducting properties of these materials have striking similarities with $CeRu_2$.

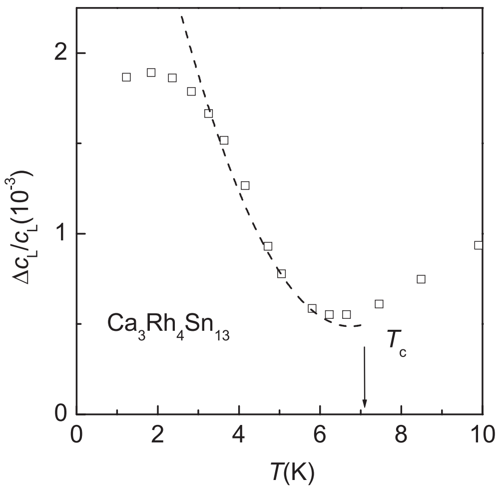

Fig. 5. c_L mode for $Yb_3Rh_4Sn_{13}$ and $Ca_3Rh_4Sn_{13}$ [13], dashed lines are fits with equation (6) using F_1 and F_2 (see text for detailes).

This is not the case for the acoustical properties because the much smaller electron – lattice coupling renders the lattice effects much smaller than for $CeRu_2$. This holds also for the ultrasonic properties in the normal state for the two classes of materials.

These two compounds were investigated acoustically by Haas et al. [13]. In the normal state the c_{44} mode shows softening of several percent from room temperature down to T_c for both compounds. The other modes, c_L and $(c_{11} - c_{12})/2$, exhibit much smaller temperature anomalies below 50 K. The various elastic modes, both longitudinal and transverse, exhibit pronounced anomalies at and below T_c. In Figure 5 we show the longitudinal elastic mode propagating in [110] $c_L = (c_{11} + c_{12} + 2c_{44})/2$ for $Ca_3Rh_4Sn_{13}$ [13]. Note that in this case we present data down to 50 mK. We found a logarithmic temperature dependence for the longitudinal modes in the low temperature range $T < 1$ K (not shown in Fig. 5). Apart from this logarithmic temperature dependence the c_L mode for $T < T_c$ can be well accounted for by F_1 and F_2.

3.6 HfV_2

This Laves phase compound, together with ZrV_2, is an interesting superconductor because of the high electronic density of states at the Fermi energy, leading to a large specific heat with a T^3 law at low temperatures. This classifies HfV_2 as a strong coupling superconductor with a high value of $\Delta C/\gamma T_c \sim 1.9$, compared to the BCS value of 1.43.

Elastic constant measurements on single crystals and polycrystals of HfV_2 showed a strong anomaly in the $(c_{11} - c_{12})/2$ mode at the structural transition of $T_a =$ 118 K [14]. Additional X-ray investigation showed the transition being from cubic to orthorhombic.

At the superconducting transition T_c one observes a clear step function anomaly for the longitudinal mode c_L and no anomaly for the transverse mode $(c_{11} - c_{12})/2$. This indicates an order parameter – strain coupling of the first term in equations (4, 6). No indications of the other higher order terms is noticeable for $T < T_c$. This behaviour is close to the behaviour of elemental superconductors or heavy fermion superconductors. Since for HfV_2 we are in the region $ql \ll 1$ we cannot observe any sound attenuation due to conduction electrons, neither for $T > T_c$ nor for $T < T_c$. In Figure 6a we show the step-function behaviour of the c_L mode at T_c together with the smooth temperature dependence of the $(c_{11} - c_{12})/2$ mode.

3.7 Heavy fermion compounds

In the heavy fermion compounds one has clear indications of strain – order parameter coupling. This is observed for both UPt_3 and URu_2Si_2 in the superconducting state [15,16] (see Fig. 6b, c).

UPt_3: Especially for UPt_3 with the complicated phase diagrams including 3 phases one clearly observes for the longitudinal elastic constants step function like behaviour as a function of temperature and magnetic field corresponding to the first term of equations (4, 6) as shown in Figure 6b. But for UPt_3 we have a multi-component order parameter. Therefore the strain–order parameter interaction and the elastic constant expressions are more complicated than discussed above. One does not find any sign of additional contributions involving F_1, F_2. The reason seems to be the large electronic Grüneisen parameter coupling observed in this case for both normal and superconducting states. Shear waves do not show any anomalies however.

URu_2Si_2: For URu_2Si_2 one also observes for longitudinal waves only strain – order parameter coupling involving g_Γ as discussed above for equations (4, 6) (see Fig. 6c). In this case the B-T phase diagram consists only of one superconducting phase. Again a strong electronic Grüneisen parameter coupling seems to explain the effects adequately, especially for the c_{11} mode [17].

$CeCu_2Si_2$: This compound exhibits also distinct lattice properties. Usually, in stoichiometric compounds, the superconducting phase is enclosed by the so-called A phase and the strain – order parameter coupling [see Eq. (6)] can account for the A-phase expulsion and superconducting phase description [18]. For non-stoichiometric $CeCu_2Si_2$ where no A phase is present one observes an ordinary step function behaviour indicating again strain-order parameter coupling of equation (6) [19] as shown in Figure 6d. In fact the temperature dependence of the c_{11} mode below T_c can be fitted quantitatively with the function F_o of equation (6). For magnetic fields $B > B_{c2} \approx 1.7$ T the step function is suppressed.

3.8 Sr_2RuO_4

The ruthenate Sr_2RuO_4 has the same layered perovskite structure of the K_2NiF_4-type as the cuprate superconductor $La_{2-x}Sr_xCuO_4$. This latter one is a d-wave superconductor. Like wise one argues that Sr_2RuO_4 is also

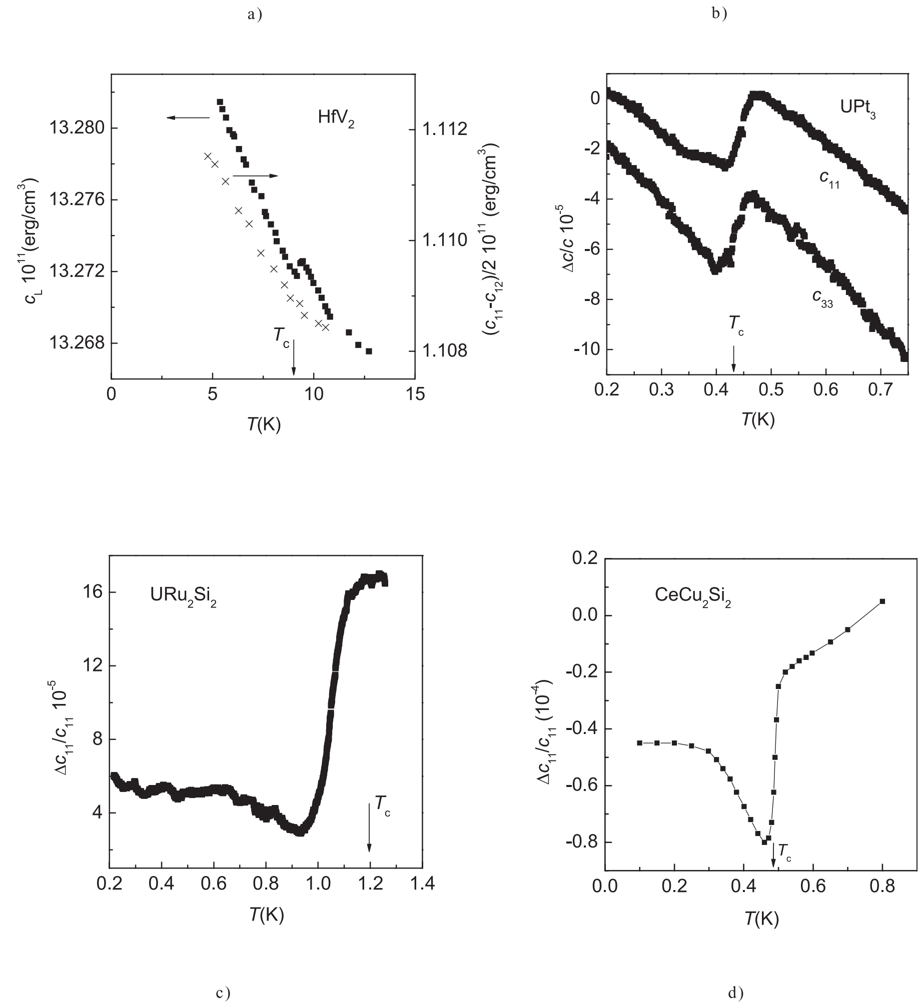

Fig. 6. a) c_L and $(c_{11} - c_{12})/2$ modes in the vicinity of T_c for HfV_2 (Ref. [14]); b) Temperature dependence of c_{11} and c_{33} modes for UPt_3 (Ref. [16]); c) Temperature dependence of c_{11} mode for URu_2Si_2 (Ref. [17]); d) $c_{11}(T)$ in $CeCu_2Si_2$ for crystal without *A*-phase [19]. Full line is a guide to the eye.

an unconventional superconductor with a *p*-wave pairing symmetry and a transition temperature $T_c = 1.42$ K [20].

Ultrasonic measurements in the superconducting state have been performed by several groups [21,22]. In addition the elastic constant tensor was determined with resonant ultrasonic spectroscopy RUS [23]. The temperature dependence of some elastic modes c_{11}, $(c_{11} - c_{12})/2$, c_{44} and c_{66} are shown in Figure 7 taken from the references listed above. In this case an order parameter-strain coupling was observed for the longitudinal mode c_{11} as for the heavy fermions and perhaps also for $(c_{11} - c_{12})/2$. In addition the other terms of equation (6) with F_1 and F_2 contribute strongly for all measured modes. The analysis of references [21,22] was made along the same lines as in this paper.

4 Discussion and conclusions

The results, presented in Figures 1–7 give a good description of the phenomenological expressions of equation (6). As fit parameters we used c_o, the background elastic constant, $(\partial T_c/\partial \varepsilon)^2 \Phi_o$ the coupling constant for the strain – order parameter coupling and the parameters A_1 and A_2. In Table 1 we have listed these parameters A_1 and A_2 which are dimensionless. As a corresponding dimensionless quantity we also list $(\Delta c/c_0)_{OP}$ which is the dimensionless step-function due to the order parameter-strain coupling, proportional to g_Γ^2, as discussed with equations (A1, A2) in the Appendix. In this way we can compare the different types of superconductors. The background elastic constant c_o is in most cases temperature independent for $T < T_c$ since T_c is small compared to the Debye temperature. However in several investigated cases, the elastic constant c_Γ, shows pronounced softening for $T > T_c$. In these cases we assume that the softening is arrested at T_c. This can be investigated by applying magnetic fields $B > B_{c2}$. Such behaviour we found for the Chevrel compounds (Fig. 2a, b), for $CeRu_2$ (Fig. 3) and for $Ca_3Rh_4Sn_{13}$ (Fig. 5). For the other compounds one could extrapolate into the $T < T_c$ region, although for some cases the situation with the background elastic constants, in particular for $T < 10$ K, should be investigated by additional experiments.

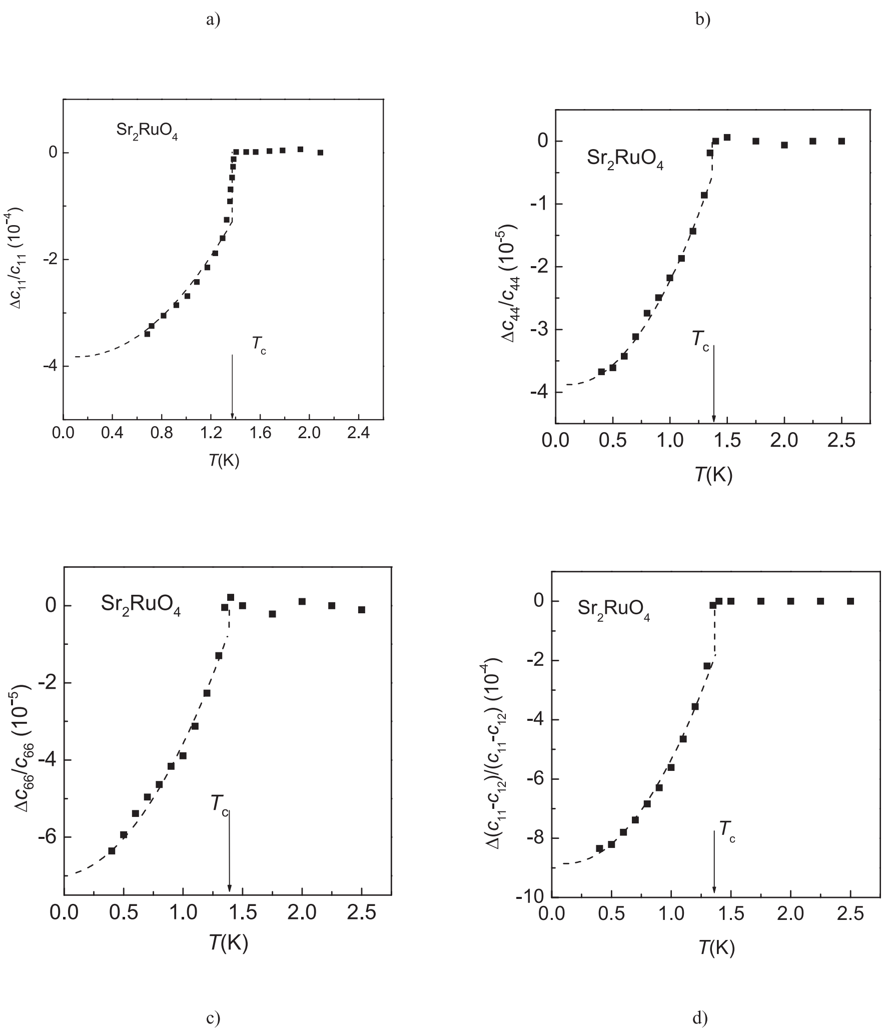

Fig. 7. Temperature dependence of different acoustic modes c_{11} (a), c_{44} (b), c_{66} (c), $c_{11} - c_{12}$ (d) in the vicinity of the superconducting transition in Sr_2RuO_4 [21,22]. Dashed lines show a fit with equation (6) for $T \leq T_c$ with parameters given in Table 1.

We see from the Figures 1–7 that only HfV_2, the heavy fermion compounds UPt_3, URu_2Si_2, $CeCu_2Si_2$ and the layer compound Sr_2RuO_4 exhibit strain-order parameter coupling effects involving the g_Γ term of equation (5), and only for longitudinal modes. The step-function at T_c for $\Delta c/c$ varies between 5×10^{-5} and 12×10^{-5} (see Fig. 6). This can be related for the heavy fermions with the large density of states at the Fermi energy E_F for these materials. Taking as a measure the Sommerfeld γ-values given in Table 1, it is evident that these materials have an observable strain-order parameter coupling. For HfV_2 the γ value is not so large, but it is considered a strong coupling superconductor. But also Sr_2RuO_4 has a relatively small γ value. Apart from the stepfunction behaviour the strain – order parameter coupling gives for $T < T_c$ a temperature dependence expressed by F_o of equation (6), as observed for $CeCu_2Si_2$ in Figure 6. It is interesting to note that shear waves may exhibit a strain – order parameter coupling [see Eq. (5)] also for multidimensional order parameters. This has been observed in Sr_2RuO_4 for the transverse modes, especially for the $(c_{11} - c_{12})$-mode [22,24] (see also Fig. 7 and Tab. 1).

Higher order terms, involving $\partial^2 T_c/\partial\varepsilon^2$ or the corresponding parameters A_1, A_2 are necessary for the fits in all discussed compounds except HfV_2 and the heavy fermions. From Table 1 we notice that A_2 is practically the same (within a factor of 2-3) for all superconductors with the exception of $Ba_{.63}K_{.37}BiO_3$ and Sr_2RuO_4, whereas A_1 is 0 for Chevrel compounds and very large for $CeRu_2$ and $Ba_{0.63}$ $K_{0.37}$ BiO_3. A_1 and A_2 involve strain derivatives of both T_c and Φ_o [see Eq. (7)]. The fits to the experimental results in Figures 1–7 shows that the strain derivatives of Φ_o are also needed (see Tab. 1).

We have treated only the field free $B = 0$ case. For $0 < B \leq B_{c2}$ pronounced dispersive effects are observed for both attenuation and velocity changes. This is especially pronounced for the Chevrel compounds and $CeRu_2$. These effects can be interpreted quantitatively with the so-called TAFF model. For a discussion of this model see reference [25].

Furthermore we have treated only elastic constant effects, neglecting attenuation effects. For all superconducting compounds discussed above we are in the limit $ql_e \ll 1$

with q the wave vector and l_e the electron mean free path. Therefore attenuation effects due to conduction electrons are completely negligible, in contrast to the elemental superconductors, with the exception of the $(c_{11} - c_{12})$-mode in Sr_2RuO_4 [21,22]. Attenuation effects in the other compounds are only observable in the presence of magnetic fields as discussed before.

High temperature cuprate superconductors have not been dealt with in this paper. The reason is either the apparent lack of pronounced sound wave effects for the $B = 0$ temperature dependence or for the La-Sr-CuO_4 the interference with a structural transition as can be seen from the magnetic field dependence (Ref. [26]). For a theoretical discussion of this class of superconductors, similar to the one given here, see reference [27].

Appendix A

Here we give the relations between the terms of equation (4) and equation (5). For illustration we consider only $T_c(\varepsilon) = T_c^0 + (\partial T_c/\partial\varepsilon)\varepsilon + (1/2)\ (\partial^2 T_c/\partial\varepsilon^2)\ \varepsilon^2$ and neglect the corresponding $\partial\Phi/\partial\varepsilon$, $\partial^2\Phi/\partial\varepsilon^2$ terms.

From equation (5) with $\Delta c_\Gamma = c_\Gamma - c_\Gamma^0 = (d^2F_{sp}/d\varepsilon^2)$ and with $(d|\eta|/d\varepsilon) = -2g\eta/(a + 3b|\eta|^2)$ we obtain

$$\Delta c_\Gamma = -2g_\Gamma^2/b + 2h_\Gamma|\eta|^2 + 2h'_\Gamma|\eta^4 + 4g'g|\eta|^2/b \quad (A.1)$$

or introducing the specific heat $\Delta C = Ta_o^2/2b = 2\Phi_o T/T_c^2$ we obtain

$$\Delta c_\Gamma = -4g_\Gamma^2\Delta C/(a_o^2 T) + 4h_\Gamma\Delta C(T_c - T)/(a_o T) + \text{higher order terms.} \quad (A.2)$$

The first term in equation (A2) is proportional to g_Γ^2 and $\Delta C/T$. The first term of equation (A1) gives a step function for $T \leq T_c$ of $\Delta c_\Gamma = -2g_\Gamma^2/b$. This we can identify with the first term of equation (4) at T_c: $\Delta c_\Gamma = -2(\partial T_c/\partial\varepsilon)^2\Phi_o/T_c^2$. Inserting Φ_0 gives $2g_\Gamma = a_o\partial T_c/\partial\varepsilon$. Equations (A1, A2) predict a stepfunction (first term) and equation (4) gives a stepfunction at T_c with a temperature dependent term below T_c. This latter term arises from the h'–term quadratic in ε_Γ of equation (5). With this comparison we can check whether we have an OP coupling of the type of equation (A1). The second term of equations (A1, A2) gives $\Delta c_\Gamma = 0$ at T_c and a temperature dependent term in T for $T < T_c$. Comparing with the second term of equation (4) we get $h = a_oT_c[4(\partial T_c/\partial\varepsilon)^2/T_c^2 - (\partial^2 T_c/\partial\varepsilon^2)/T_c]/4$ and corresponding expressions for the constants g' and h'. In the following equation (A3) we collect these expressions, where we have only considered $T_c(\varepsilon)$:

$$g_\Gamma = -(a_0/2)\partial T_c/\partial\varepsilon_\Gamma \qquad g'_\Gamma = (b/2T_c)\partial T_c/\partial\varepsilon_\Gamma$$
$$h_\Gamma = (a_oT_c/4)[4(\partial T_c/\partial\varepsilon_\Gamma)^2/T_c^2 - \partial^2 T_c/\partial\varepsilon_\Gamma^2/T_c]$$
$$h'_\Gamma = (b/4)[-3(\partial T_c/\partial\varepsilon_\Gamma)^2/T_c^2 + (\partial^2 T_c/\partial\varepsilon_\Gamma^2)/T_c]. \quad (A.3)$$

Similar expressions can be gained for the other terms involving derivatives of Φ_o. We see that we can interpret the terms involving the strain derivatives of T_c and Φ_o with this Landau strain expansion (Eq. (5)) quantitatively. A similar analysis was made using the two-fluid model of superconductivity [21,22].

References

1. B. Lüthi *Physical Acoustics in the Solid State* (Springer, Heidelberg, 2005)
2. L.R. Testardi, Rev. Mod. Phys. **47**, 637 (1975); L.R. Testardi, *Physical Acoustics*, Vol. X (Acad. Press, 1974)
3. A.B. Pippard, Phil. Mag. **46**, 1115 (1955)
4. L.R. Testardi, Phys. Rev. B **3**, 95 (1971)
5. W. Rehwald, Phys. Lett. **27**A, 287 (1968)
6. O. Fischer, Appl. Phys. **16**, 1 (1978)
7. O. Pena, M. Sergent, Progr. Solid State Chem. **19**, 165 (1989)
8. B. Wolf et al., Phys. Rev. B **54**, 348 (1996)
9. H. Goshima et al., Physica B **223&224**, 172 (1996)
10. B. Wolf et al., J. Low Temp. Phys. **107**, 421 (1997)
11. M. Yoshizawa et al., J. Phys. Soc. Jpn. **66**, 2355 (1997)
12. S. Zherlitsyn et al., Eur. Phys. J. B **16**, 59 (2000)
13. A. Haas et al., J. Low Temp. Phys. **114**, 285 (1999)
14. B. Lüthi et al., Z. Phys. B **60**, 387 (1985)
15. G. Bruls et al., Phys. Rev. Lett. **65**, 2294 (1990); S. Addenwalla et al., Phys. Rev. Lett. **65**, 2298 (1990)
16. P. Thalmeier et al., Physica C **175**, 61 (1991)
17. B. Wolf et al., J. Low Temp. Phys. **94**, 307 (1994)
18. G. Bruls et al., Phys. Rev. Lett. **72**, 1754 (1994)
19. D. Finsterbusch, Ph.D. thesis Universität Frankfurt (2003)
20. Y. Maeno, T.M. Rice, M. Sigrist, Physics Today, January 2001, p. 42
21. H. Matsui et al., J. Phys. Soc. Jpn. **63**, 060505 (2001)
22. N. Okuda et al., J. Phys. Soc. Jpn. **71**, 1134 (2002)
23. J. Paglione et al., Phys. Rev. B **65**, 220506 (2002)
24. M. Sigrist, Progr. Theor. Phys. **107**, 917 (2002)
25. J. Pankert, Physica C **168**, 335 (1990)
26. T. Suzuki et al., J. Supercond. **7**, 419, 1994; T. Hanaguri et al. Physica C **185-189**, 1395 (1991)
27. A.J. Millis, K.M. Rabe, Phys. Rev. B **38**, 8908 (1988)